Electrothermal Transistor Effect and Cyclic Electronic Currents in Multithermal Charge Transfer Networks

Galen T. Craven[1,*] and Abraham Nitzan[1,2,†]
[1]Department of Chemistry, University of Pennsylvania, Philadelphia, Pennsylvania 19104, USA
[2]School of Chemistry, Tel Aviv University, Tel Aviv 69978, Israel

(Received 10 December 2016; revised manuscript received 24 February 2017; published 15 May 2017)

A theory is developed to describe the coupled transport of energy and charge in networks of electron donor-acceptor sites which are seated in a thermally heterogeneous environment, where the transfer kinetics are dominated by Marcus-type hopping rates. It is found that the coupling of heat and charge transfer in such systems gives rise to exotic transport phenomena which are absent in thermally homogeneous systems and cannot be described by standard thermoelectric relations. Specifically, the directionality and extent of thermal transistor amplification and cyclical electronic currents in a given network can be controlled by tuning the underlying temperature gradient in the system. The application of these findings toward the optimal control of multithermal currents is illustrated on a paradigmatic nanostructure.

DOI: 10.1103/PhysRevLett.118.207201

The coupling between electron transfer (ET) and transport and the underlying thermal environment is a long-studied subject [1]. Its manifestations in recent studies of transport in molecular junctions mostly focus on the weak electron-phonon coupling regime. Similarly, thermoelectric phenomena in such junctions [2], where molecules connect between electrodes of different temperatures, are usually treated (with a few exceptions, e.g., Refs. [3–12]) with the electron-vibration interaction disregarded. This stands in contrast to electron transfer reactions in condensed molecular systems that are usually dominated by hopping between thermally equilibrated polaronlike states as described by Marcus theory [13–16] (analogous kinetics in junction transport is known, mostly in so-called redox molecular junctions [17,18]). We have recently considered the latter type of electronic transport in thermally heterogeneous systems, where an electron hops between two sites of different local temperatures [19]. This study was motivated by recent advances in the measurement and control of temperature differences on length scales comparable to those involved in molecular electron transfer processes [20–25]. The corresponding ET rate was obtained as a modified multidimensional Marcus expression that depends on the local temperatures of the two sites. Furthermore, electron hopping was shown to be accompanied by heat transfer between the sites whose magnitude depends on the temperature difference and on the reorganization (polaron formation) energies at the two sites.

Thermal inhomogeneity can develop spontaneously in driven nonequilibrium systems [26–30] or can be externally controlled as in a thermoelectric device. Considering such models, several recent theoretical studies have discovered interesting thermal transistor effects, whereupon the flux between two sites can be controlled by the temperature on a third site [31–33].

In this Letter, we develop a theory to describe ET in complex networks of donor-acceptor sites, where each site is associated with normal modes that are in contact with an independent heat bath at the local site temperature. This is an idealization of the standard phenomenology of molecular electron transfer where the electronic processes is most strongly coupled to vibrations that are localized on the donor and acceptor sites. In the limit of strong electron-phonon coupling, electron transport is dominated by hopping-type events, and the Marcus theory gives the conceptual basis, and sometimes quantitative understanding, of ET reactions [13–16]. The multithermal nature of the examined systems arises because the donor and acceptor sites can be at different temperatures. Purely vibrational heat transfer between sites is disregarded for simplicity, so in what follows we focus on electron transfer and the associated heat transfer [19,34]. The development of complex network theory [35] has significantly increased our understanding of the flow of charge, energy, and information in diverse types of systems [36–45], and the present study makes it possible to consider electron and heat transport within such a framework and to study the consequence of their interdependence.

The donor-acceptor networks we consider consist of S sites, where each site s, which has local temperature T_s, is associated with N_s harmonic modes that are equilibrated with the thermal environment about that site. Specifically, we consider transitions between electronic states for which an excess electron is localized on different sites of this network. In the Marcus picture [13] of ET, the localized occupation of electron density associated with electronic state a of the network is described by the energy surface

$$E_a(x_1,\ldots,x_N) = E_a^{(0)} + \sum_s^S \sum_{j\in\mathcal{M}^{(s)}} \frac{1}{2} k_j \left(x_j - \lambda_j^{(a)}\right)^2, \quad (1)$$

where $E_a^{(0)}$ is an electronic energy origin of state a, x_j is the coordinate of the jth vibrational mode, and $\lambda_j^{(a)}$ is a shift in the equilibrium position of the jth mode. Both $E_a^{(0)}$ and $\lambda_j^{(a)}$ are measured relative to some reference state for which $E_{\mathrm{ref}}^{(0)}$ and $\lambda_j^{(\mathrm{ref})}$ vanish (properties of this state do not affect the final results). The total number of modes in the system is denoted by $N = \sum_s^S N_s$, and the group of N_s modes associated with the sth site is denoted $\mathcal{M}^{(s)}$. In a likely special case, $\lambda_j^{(a)} = 0$ unless mode j is localized about the site on which the electron is placed in state a (that is, unless $j \in \mathcal{M}^{(s)}$ and a is the electronic state that corresponds to the electron occupying site s). However, the form (1) can represent more general situations where the modes localized about site s respond to the electronic occupation on a different site. A transition between states a and b is associated with a reorganization energy (assumed temperature independent) in the jth mode, $E_{Rj}^{(a,b)}$, and a total reorganization energy $E_R^{(a,b)}$, which are given by

$$E_{Rj}^{(a,b)} = \frac{1}{2} k_j \left(\lambda_j^{(a)} - \lambda_j^{(b)}\right)^2 \quad \text{and} \quad E_R^{(a,b)} = \sum_j^N E_{Rj}^{(a,b)}. \tag{2}$$

The shifts λ, and hence the reorganization energies, depend on the intersite distances and therefore the topology of the underlying connectivity network. Shown in Fig. 1 are representative topologies for three typical connectivities: ring $\mathcal{R}$, linear $\mathcal{L}$, and complete $\mathcal{K}$. Associated with each network is an adjacency matrix $\mathbf{A}$ where $A_{ab} = 1$ if sites a and b are connected (and thus the electron can tunnel between sites) and is zero otherwise [35]. The topology of $\mathbf{A}$ determines which modes are responsive to electron

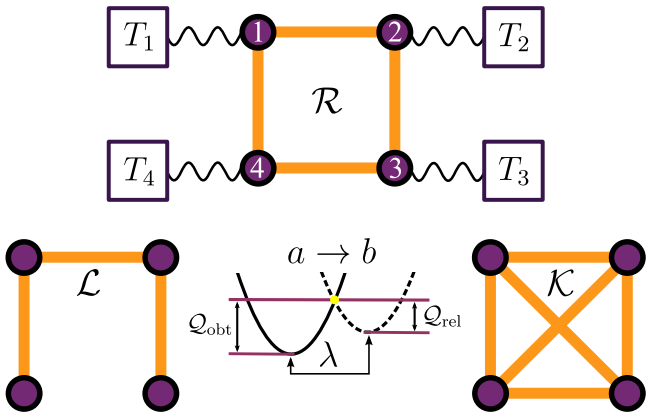

FIG. 1. Network graphs for $\mathcal{R}$, $\mathcal{L}$, and $\mathcal{K}$ topologies. Each node represents a donor-acceptor site. As shown explicitly in the $\mathcal{R}$ graph, each site is in contact with an independent thermal bath. The center panel shows a schematic of the energy surfaces E_a (solid curve) and E_b (dashed curve) and $\mathcal{Q}_{\mathrm{obt}}$ and $\mathcal{Q}_{\mathrm{rel}}$ for the state transition $a \to b$.

localization on a particular site. We next show that temperature differences between sites give rise to emergent and sometimes exotic thermal and electronic transport properties.

The electron transfer rate between any two sites in the network and the heat transfer rate between the thermal baths involved in this transition can be derived by adopting the formalism put forth in Ref. [19] for bithermal electron hopping between two sites. "Involved bath" implies that the harmonic modes that are thermalized by this bath are sensitive to the electronic population of at least one of the sites. Under standard transition state theory assumptions, the rate of the $a \to b \equiv a, b$ transition can be expressed as

$$k_{a,b} = \frac{1}{2} \langle \mathcal{T}_{a,b} \dot{x}_\perp \rangle P_{a,b}, \tag{3}$$

where $\mathcal{T}_{a,b}$ is the tunneling probability between states, $P_{a,b}$ is the probability density about a transition surface (TS) separating the states, both evaluated on the E_a surface, and $\dot{x}_\perp$ is the velocity in the direction normal to the TS [46,47]. The normal velocity $\dot{x}_\perp = \dot{\mathbf{x}} \cdot \hat{\mathbf{u}}_\perp(\mathbf{x})$, where $\hat{\mathbf{u}}_\perp(\mathbf{x})$ is a unit vector normal to the TS at position $\mathbf{x}$ on this hypersurface. The factor $\langle \mathcal{T}_{a,b} \dot{x}_\perp \rangle$ is a (multi)thermal average that depends on the temperature of each bath involved in the transition. The TS is determined by the requirement that a transition can take place only at nuclear configurations where electronic energy is conserved. For the N-dimensional paraboloid energy surface defined by (1), the TS separating states is an $(N-1)$-dimensional transition state hypersurface which is the locus of mode configurations where $E_a = E_b$, defined by $g_c(x_1, \ldots, x_N) = E_b(x_1, \ldots, x_N) - E_a(x_1, \ldots, x_N)$.

In the adiabatic limit of the Marcus rate theory, $\mathcal{T}_{a,b} = 1$, and the preexponential factor is proportional to $\langle \dot{x}_\perp \rangle$ [48]. In the nonadiabatic limit [49], $\mathcal{T}_{a,b}$ can be approximated by the corresponding limit of the Landau-Zener expression [15,50,51] which is evaluated in the direction normal to the TS [52]. In this limit, $\mathcal{T}_{a,b} \propto 1/\dot{x}_\perp$, and the expectation value $\langle \mathcal{T}_{a,b} \dot{x}_\perp \rangle$ does not depend on the normal velocity [53]. For the $a \to b$ transition, the multithermal probability to be on the TS is

$$P_{a,b} = \int_{\mathbb{R}^N} |\nabla g_c| \delta(g_c(x_1, \ldots, x_N)) \times \prod_s^S \prod_{j \in \mathcal{M}^{(s)}} \exp\left[-\beta_s \frac{k_j}{2} \left(x_j - \lambda_j^{(a)}\right)^2\right] dx_j \Bigg/ \int_{\mathbb{R}^N} \prod_s^S \prod_{j \in \mathcal{M}^{(s)}} \exp\left[-\beta_s \frac{k_j}{2} \left(x_j - \lambda_j^{(a)}\right)^2\right] dx_j, \tag{4}$$

where $\beta_s = 1/k_B T_s$ with k_B being the Boltzmann constant. The δ function in (4) constrains the integration over the vibrational subspace in which $E_a = E_b$, and the gradient magnitude $|\nabla g_c| = \sqrt{\sum_j^N 2 k_j E_{Rj}^{(a,b)}}$ gives a precise definition to this constraint [54,55]. Evaluating the integrals in Eq. (4), we obtain

$$P_{a,b} = \sqrt{\sum_j^N k_j E_{Rj}^{(a,b)} \Big/ 2\pi k_B \sum_s^S T_s \sum_{j\in\mathcal{M}^{(s)}} E_{Rj}^{(a,b)}} \times \exp\left[-\left(E_{ba} + E_R^{(a,b)}\right)^2 \Big/ 4k_B \sum_s^S T_s \sum_{j\in\mathcal{M}^{(s)}} E_{Rj}^{(a,b)}\right], \tag{5}$$

which expresses the probability density on the reaction path in terms of the temperature of each bath, and the reorganization energy and reaction free energy $E_{ba} = -E_{ab} = E_b^{(0)} - E_a^{(0)}$ of the respective transition. In the uniform temperature limit, combining Eqs. (3) and (5) recovers the Marcus rate [13–16].

With the multidimensional-multithermal transition rate $k_{a,b}$ now derived, the kinetic equations for the occupation probability $\mathcal{P}$ of each state can be constructed. For a reaction network (see Fig. 1) with adjacency matrix $\mathbf{A}$, these equations take the form

$$\frac{d\mathcal{P}_a}{dt} = \sum_b A_{ba} k_{b,a} \mathcal{P}_b(t) - A_{ab} k_{a,b} \mathcal{P}_a(t) \tag{6}$$

for each state a. At steady state, $d\mathcal{P}_a/dt = 0\,\forall\, a$, which implies that the net electronic flux between sites vanishes.

Next consider the heat transfer associated with a given electron transfer step [19,56]. In Marcus theory, the nuclear motion leading to the $a \to b$ transition proceeds through a point $\boldsymbol{x}^{\mathrm{TS}}$ on the TS, and the corresponding heat transferred into a specific bath during the transition is $\mathcal{Q}^{(a,b)}(\boldsymbol{x}^{\mathrm{TS}}) = -\mathcal{Q}^{(a)}_{\mathrm{obt}}(\boldsymbol{x}^{\mathrm{TS}}) + \mathcal{Q}^{(b)}_{\mathrm{rel}}(\boldsymbol{x}^{\mathrm{TS}})$, where the first term is the heat obtained from the bath during the ascent to $\boldsymbol{x}^{\mathrm{TS}}$ on the E_a surface and the second term is the heat released to the bath during the descent to equilibrium on the E_b surface (see Fig. 1). Using the energy surfaces of Eq. (1), the contribution of mode j to the net heat exchange with the bath associated with it during the $a \to b$ transition is given by

$$\mathcal{Q}_j^{(a,b)} = -\frac{1}{2}k_j\left[x_j^{\mathrm{TS}} - \lambda_j^{(a)}\right]^2 + \frac{1}{2}k_j\left[x_j^{\mathrm{TS}} - \lambda_j^{(b)}\right]^2. \tag{7}$$

This quantity should be averaged over the probability to reach the particular configuration on the TS when coming from the a side:

$$\left\langle \mathcal{Q}_j^{(a,b)} \right\rangle = \int_{\mathbb{R}^N} \mathcal{Q}_j^{(a,b)} P^{\ddagger}_{a,b}(x_1, \ldots, x_N) dx_1 \ldots dx_N, \tag{8}$$

where $P^{\ddagger}_{a,b}$ is the probability density on the TS when the system is in state a [48]:

$$P^{\ddagger}_{a,b} = \delta(g_c) \prod_s^S \prod_{j\in\mathcal{M}^{(s)}} \exp\left[-\beta_s \frac{1}{2}k_j\left(x_j - \lambda_j^{(a)}\right)^2\right] \Big/ \int_{\mathbb{R}^N} \delta(g_c) \prod_s^S \prod_{j\in\mathcal{M}^{(s)}} \exp\left[-\beta_s \frac{1}{2}k_j\left(x_j - \lambda_j^{(a)}\right)^2\right] dx_j. \tag{9}$$

Evaluating the expectation integral gives

$$\left\langle \mathcal{Q}_j^{(a,b)} \right\rangle = \frac{E_{Rj}^{(a,b)}\left(E_{ab}T_j + \sum_{k\neq j}^N E_{Rk}^{(a,b)}(T_k - T_j)\right)}{\sum_k^N T_k E_{Rk}^{(a,b)}}, \tag{10}$$

where $T_j = T_s$ if $j \in \mathcal{M}^{(s)}$. The total heat transferred to the thermal environment of site s during the $a \to b$ transition is the sum of contributions over all modes associated with that site:

$$\left\langle \mathcal{Q}_s^{(a,b)} \right\rangle = \frac{\sum_{j\in\mathcal{M}^{(s)}} E_{Rj}^{(a,b)}\left(E_{ab}T_s + \sum_{q\neq s}^S \sum_{k\in\mathcal{M}^{(q)}} E_{Rk}^{(a,b)}(T_q - T_s)\right)}{\sum_q^S T_q \sum_{k\in\mathcal{M}^{(q)}} E_{Rk}^{(a,b)}}. \tag{11}$$

Here, the term proportional to E_{ab} expresses the heat released to or taken from the baths from the free energy difference between these electronic states, while the term proportional to $(T_q - T_s)$ is the actual heat transfer between baths q and s associated with the $a \to b$ transition.

The heat current into the thermal environment of site s is

$$\frac{d\mathcal{Q}_s}{dt} = \sum_{a,b} A_{ab} k_{a,b} \mathcal{P}_a(t) \left\langle \mathcal{Q}_s^{(a,b)} \right\rangle. \tag{12}$$

Note that, while $\mathcal{P}_a(t) \geq 0\,\forall\, t$, the expectation value of $\mathcal{Q}_s^{(a,b)}$ and the heat current $\dot{\mathcal{Q}}_s$ can be either positive or negative, implying that the corresponding bath absorbs or releases energy, respectively. In unithermal systems at steady state, the heat currents vanish ($\dot{\mathcal{Q}}_s = 0\,\forall\, s$), while in contrast, for multithermal systems, $\langle \mathcal{Q}_s \rangle \neq 0$ and thus $\dot{\mathcal{Q}}_s \neq 0$. Note that, even as the occupation probabilities approach electronic quasiequilibrium where the net electronic currents are zero, the net flow of heat between sites does not vanish. This phenomenon is not a standard thermoelectric effect and reveals a novel pathway for energy transport in multithermal charge transfer networks.

Another interesting behavior that is observed in multithermal networks with closed loops is the persistence of steady-state net electronic bond currents $\mathcal{J}_{a,b} - \mathcal{J}_{b,a} = k_{a,b}\mathcal{P}_a - k_{b,a}\mathcal{P}_b$, i.e., the breaking of detailed balance, and the formation of cyclical current loops that obviously

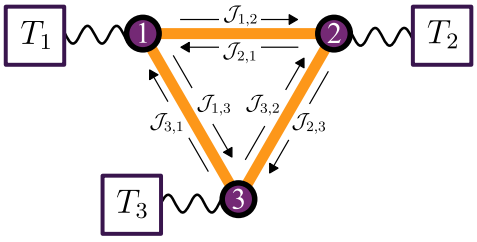

FIG. 2. Network graph for a three-site ring ($\mathcal{R}_3$) network.

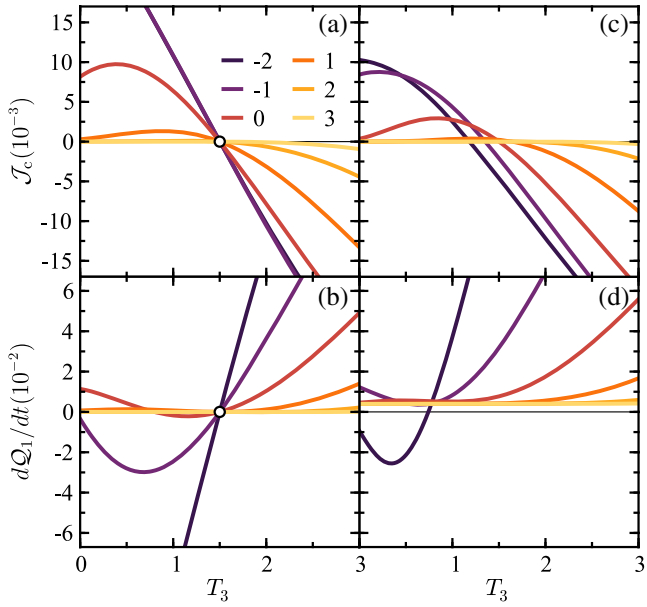

FIG. 3. Cyclic flux $\mathcal{J}_c$ (top) and heat current $d\mathcal{Q}_1/dt$ (bottom) in the nonadiabatic limit as functions of T_3 for a three-site $\mathcal{R}_3$ network. Each curve corresponds to the respective value of $E_3^{(0)}$ marked in the legend. In each panel, $E_1^{(0)} = -4$, $E_2^{(0)} = 0$, and $T_2 = 3/2$ with (a),(b) $T_1 = 3/2$ and (c),(d) $T_1 = 3/4$. The circular markers denote unithermal points. All reorganization energies are $E_{Rj} = 1/2$ for each mode involved in a particular transition and zero otherwise. All quantities are shown in reduced units [53,60].

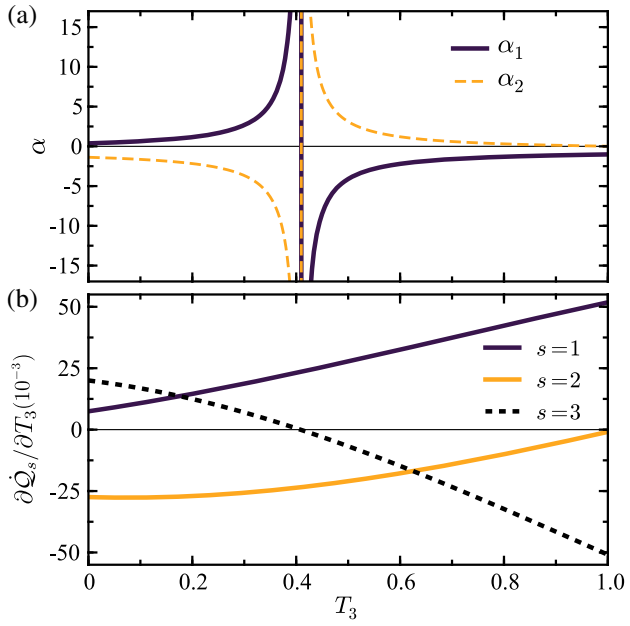

FIG. 4. (a) Amplification factor α and (b) heat current derivatives $\partial\dot{\mathcal{Q}}_s/\partial T_3$ as functions of T_3 for a multithermal $\mathcal{R}_3$ system with $T_1 = 3/4$, $T_2 = 3/2$, and $E_{Rj} = 1/2\,\forall\, j$ over each state transition. In both panels, $E_1^{(0)} = -4$ and $E_2^{(0)} = E_3^{(0)} = 0$.

vanish in full equilibrium where detailed balance is maintained. An example is seen in the three-site ring ($\mathcal{R}_3$) shown in Fig. 2. We emphasize this simple system because of its experimental realizability and its general applications in molecular electronics and devices [33,57,58], but note that other more complex networks can also be analyzed using the developed theory [59]. In a multithermal $\mathcal{R}_3$ network, the direction and magnitude of the cyclic flux $\mathcal{J}_c = \mathcal{J}_{1,2} - \mathcal{J}_{2,1} = \mathcal{J}_{2,3} - \mathcal{J}_{3,2} = \mathcal{J}_{3,1} - \mathcal{J}_{1,3}$ can be altered by tuning the temperature T_3. This is illustrated in Fig. 3(a), where the donor-acceptor sites 1 and 2 are at the same temperature while variation of the temperature on another site, T_3, determines the direction and magnitude of the cyclical current. We find that this thermally induced current persists, except in the case that the electronic occupation energy $E_a^{(0)}$ is the same for all sites involved in the cycle. Note that, at the unithermal point in Figs. 3(a) and 3(b), $\mathcal{J}_{a,b} = \mathcal{J}_{b,a}$ for every connection, so $\mathcal{J}_c = 0$. This is simply a statement that with no temperature gradient there is no heat current or cyclic electron flux. Similar trends are also observed in Figs. 3(c) and 3(d) for networks where the local temperature of each site is different. By comparing the temperatures at which $\mathcal{J}_c = 0$ in Fig. 3(c) with the heat currents at the same temperature in Fig. 3(d), it can be seen that even when the electron flux vanishes there is still a net heat flow between baths. At full equilibrium, which is achieved in the uniform temperature limit, all electronic and heat fluxes vanish.

The theory of coupled electron and heat transfer developed in this Letter can also be applied to elucidate the electronic contribution to transport phenomena in thermal transistors [31–33], which are recently studied model devices that can be used to control and amplify heat flow. Following Ref. [31], we quantify the magnitude of amplification in thermal transistors by the factor $\alpha_s = \partial\dot{\mathcal{Q}}_s/\partial\dot{\mathcal{Q}}_3 : s \in \{1, 2\}$, which measures the effect of pumping heat into site 3 on the heat current between sites 1 and 2. If $|\alpha_s| > 1$, a transistor effect is present. In the three-site $\mathcal{R}_3$ system, variation of the heat current $\dot{\mathcal{Q}}_3$ by an alteration of T_3 can give rise to significant amplifications, as shown in Fig. 4(a). The reason for the electrothermal transistor effect is shown in Fig. 4(b), where $\partial\dot{\mathcal{Q}}_3/\partial T_3 \to 0$ at $T_3 \approx 0.4$ while $|\partial\dot{\mathcal{Q}}_s/\partial T_3| \gg \partial\dot{\mathcal{Q}}_3/\partial T_3$ for $s \in \{1, 2\}$ as this limit is approached. This aligns with the region of amplification shown in Fig. 4(a).

We have shown that, in nanoscale systems where localized modes are in contact with environments at different temperatures, complex nonlinearities in the thermal gradient can induce currents which are characterized by multiple temperatures. A theory has been developed to unify the description of heat and charge transfer in these systems with multithermal temperature gradients between donor-acceptor states. This work provides a bridge connecting theories of electron transfer, heat transport, and thermoelectricity in systems where electron transport is dominated by intersite hopping and will be useful in the

design of electronic and thermoelectric devices that operate in this limit.

In regimes where the magnitude of heat conduction due to electron transport dominates over the magnitude of conduction from phonons, the developed theory will be directly applicable. Otherwise, a complete picture of the conduction process will require a theory that considers both electrothermal and phononic heat transport and their coupling. The examination of thermopower, efficiency, and their relation to electrothermal transport in molecular junctions (and other complex donor-acceptor networks with molecule-metal and molecule-semiconductor interfaces) in the phonon-assisted hopping limit of electronic transport is a potential application of the present theory [56,61,62]. Generalizations that go beyond the semiclassical Marcus treatment are obviously needed and will be taken on in future work.

A. N. is supported by the Israel Science Foundation, the U.S.–Israel Binational Science Foundation, and the University of Pennsylvania.

*gcraven@sas.upenn.edu
†anitzan@sas.upenn.edu

[1] M. Galperin, M. A. Ratner, and A. Nitzan, J. Phys. Condens. Matter **19**, 103201 (2007).
[2] Y. Dubi and M. Di Ventra, Rev. Mod. Phys. **83**, 131 (2011).
[3] K. Walczak, Physica (Amsterdam) **392B**, 173 (2007).
[4] M. Galperin, A. Nitzan, and M. A. Ratner, Mol. Phys. **106**, 397 (2008).
[5] Y. Wang, J. Zhou, and R. Yang, J. Phys. Chem. C **115**, 24418 (2011).
[6] J. Ren, J.-X. Zhu, J. E. Gubernatis, C. Wang, and B. Li, Phys. Rev. B **85**, 155443 (2012).
[7] M. B. Tagani and H. R. Soleimani, J. Appl. Phys. **112**, 103719 (2012).
[8] M. B. Tagani and H. R. Soleimani, Physica (Amsterdam) **413B**, 86 (2013).
[9] C. A. Perroni, D. Ninno, and V. Cataudella, Phys. Rev. B **90**, 125421 (2014).
[10] C. A. Perroni, D. Ninno, and V. Cataudella, New J. Phys. **17**, 083050 (2015).
[11] T. Koch, J. Loos, and H. Fehske, Phys. Rev. B **89**, 155133 (2014).
[12] N. A. Zimbovskaya, J. Phys. Condens. Matter **28**, 183002 (2016).
[13] R. A. Marcus, J. Chem. Phys. **24**, 966 (1956).
[14] R. A. Marcus, Annu. Rev. Phys. Chem. **15**, 155 (1964).
[15] A. Nitzan, *Chemical Dynamics in Condensed Phases: Relaxation, Transfer, and Reactions in Condensed Molecular Systems* (Oxford University, New York, 2006).
[16] B. Peters, J. Phys. Chem. B **119**, 6349 (2015).
[17] J. Zhang, A. M. Kuznetsov, I. G. Medvedev, Q. Chi, T. Albrecht, P. S. Jensen, and J. Ulstrup, Chem. Rev. **108**, 2737 (2008).
[18] A. Migliore and A. Nitzan, J. Am. Chem. Soc. **135**, 9420 (2013).
[19] G. T. Craven and A. Nitzan, Proc. Natl. Acad. Sci. U.S.A. **113**, 9421 (2016).
[20] C. W. Chang, D. Okawa, A. Majumdar, and A. Zettl, Science **314**, 1121 (2006).
[21] S. Sadat, A. Tan, Y. J. Chua, and P. Reddy, Nano Lett. **10**, 2613 (2010).
[22] J. A. Malen, S. K. Yee, A. Majumdar, and R. A. Segalman, Chem. Phys. Lett. **491**, 109 (2010).
[23] A. Tan, J. Balachandran, S. Sadat, V. Gavini, B. D. Dunietz, S.-Y. Jang, and P. Reddy, J. Am. Chem. Soc. **133**, 8838 (2011).
[24] W. Lee, K. Kim, W. Jeong, L. A. Zotti, F. Pauly, J. C. Cuevas, and P. Reddy, Nature (London) **498**, 209 (2013).
[25] Y. Kim, W. Jeong, K. Kim, W. Lee, and P. Reddy, Nat. Nanotechnol. **9**, 881 (2014).
[26] A. V. Popov and R. Hernandez, J. Chem. Phys. **126**, 244506 (2007).
[27] C. Jarzynski, Nat. Phys. **11**, 105 (2015).
[28] G. T. Craven and R. Hernandez, Phys. Rev. Lett. **115**, 148301 (2015).
[29] Q. Li, I. Duchemin, S. Xiong, G. C. Solomon, and D. Donadio, J. Phys. Chem. C **119**, 24636 (2015).
[30] M. Einax and A. Nitzan, J. Chem. Phys. **145**, 014108 (2016).
[31] B. Li, L. Wang, and G. Casati, Appl. Phys. Lett. **88**, 143501 (2006).
[32] P. Ben-Abdallah and S.-A. Biehs, Phys. Rev. Lett. **112**, 044301 (2014).
[33] K. Joulain, J. Drevillon, Y. Ezzahri, and J. Ordonez-Miranda, Phys. Rev. Lett. **116**, 200601 (2016).
[34] D. V. Matyushov, Proc. Natl. Acad. Sci. U.S.A. **113**, 9401 (2016).
[35] J. Schnakenberg, Rev. Mod. Phys. **48**, 571 (1976).
[36] S. H. Strogatz, Nature (London) **410**, 268 (2001).
[37] R. Albert and A.-L. Barabási, Rev. Mod. Phys. **74**, 47 (2002).
[38] E. Estrada and N. Hatano, Chem. Phys. Lett. **439**, 247 (2007).
[39] J. Gao, S. V. Buldyrev, S. Havlin, and H. E. Stanley, Phys. Rev. Lett. **107**, 195701 (2011).
[40] G. C. Solomon, C. Herrmann, T. Hansen, V. Mujica, and M. A. Ratner, Nat. Chem. **2**, 223 (2010).
[41] D. Rai, O. Hod, and A. Nitzan, J. Phys. Chem. Lett. **2**, 2118 (2011).
[42] D. Rai, O. Hod, and A. Nitzan, Phys. Rev. B **85**, 155440 (2012).
[43] B. M. Savoie, K. L. Kohlstedt, N. E. Jackson, L. X. Chen, M. Olvera de la Cruz, G. C. Schatz, T. J. Marks, and M. A. Ratner, Proc. Natl. Acad. Sci. U.S.A. **111**, 10055 (2014).
[44] M. Einax and A. Nitzan, J. Phys. Chem. C **118**, 27226 (2014).
[45] T. Hansen and G. C. Solomon, J. Phys. Chem. C **120**, 6295 (2016).
[46] S. Hammes-Schiffer and J. C. Tully, J. Chem. Phys. **103**, 8528 (1995).

[47] G. H. Jóhannesson and H. Jónsson, J. Chem. Phys. **115**, 9644 (2001).
[48] See Supplemental Material at http://link.aps.org/supplemental/10.1103/PhysRevLett.118.207201 for detailed derivations of each component in the rate and heat transfer expressions.
[49] For experimental setups in which sites of appreciably different temperatures are relatively far from each other, implying relatively weak electronic coupling, the nonadiabatic limit will be the most pertinent.
[50] D. L. Thompson, *Modern Methods for Multidimensional Dynamics Computations in Chemistry* (World Scientific, Singapore, 1998).
[51] A. O. Lykhin, D. S. Kaliakin, G. E. dePolo, A. A. Kuzubov, and S. A. Varganov, Int. J. Quantum Chem. **116**, 750 (2016).
[52] A. J. Marks and D. L. Thompson, J. Chem. Phys. **96**, 1911 (1992).
[53] In the nonadiabatic limit, a coupling constant between diabatic surfaces, $H_{a,b} = 0.01$ eV, has been used in all calculations.
[54] E. Vanden-Eijnden and F. A. Tal, J. Chem. Phys. **123**, 184103 (2005).
[55] C. Hartmann, J. C. Latorre, and G. Ciccotti, Eur. Phys. J. Spec. Top. **200**, 73 (2011).
[56] G. T. Craven and A. Nitzan, J. Chem. Phys. **146**, 092305 (2017).
[57] N. Li, J. Ren, L. Wang, G. Zhang, P. Hänggi, and B. Li, Rev. Mod. Phys. **84**, 1045 (2012).
[58] A. E. Allahverdyan, S. G. Babajanyan, N. H. Martirosyan, and A. V. Melkikh, Phys. Rev. Lett. **117**, 030601 (2016).
[59] An analysis of electric and heat currents for other multithermal networks is given in Supplemental Material [48].
[60] Characteristic units are $\epsilon = 0.02$ eV for energy, $\tau = 0.5$ ps for time, and $\sigma = 1$ nm for length. Using these units, a reduced temperature of $k_B T/\epsilon \approx 1.3$ corresponds to $T = 300$ K.
[61] C. Jia *et al.*, Science **352**, 1443 (2016).
[62] A. G. Gagorik, B. Savoie, N. Jackson, A. Agrawal, A. Choudhary, M. A. Ratner, G. C. Schatz, and K. L. Kohlstedt, J. Phys. Chem. Lett. **8**, 415 (2017).